https://doi.org/10.1016/j.apenergy.2017.03.019 This is the Pre-Published Version.

Comparison of energy performance between PV double skin facades and PV insulating glass units

Meng Wang[a], Jinqing Peng[a,*], Nianping Li[a,**], Hongxing Yang[b], Chunlei Wang[a], Xue Li[a], Tao Lu[c]

[a] *College of Civil Engineering, Hunan University, Changsha 410082, Hunan, China*

[b] *Renewable Energy Research Group (RERG), Department of Building Services Engineering, The Hong Kong Polytechnic University, Hong Kong, China*

[c] *BYD Company limited, Shenzhen 518116, Guangdong, China*

*Corresponding author. Tel.: +86 731 84846217; Email address: Jallenpeng@gmail.com (J. Peng).

**Corresponding author. Tel.: +86 731 88822667; Email address: linianping@126.com (N. Li).

Abstract

Building-integrated photovoltaic (BIPV) windows provide the benefits of generating electricity, reducing building cooling and heating energy consumption, and efficiently utilizing daylight simultaneously. In this paper, the overall energy performance of a PV double skin façade (PV-DSF) and a PV insulating glass unit (PV-IGU) is studied through comparative experiments on a test rig in Hong Kong. The PV-DSF means ventilated PV-DSF by default, if not special mentioned. It is found that the average solar heat gain coefficients (SHGCs) of the PV-DSF and the PV-IGU are 0.152 and 0.238, while the U-values are 2.535 W/m^2 K and 2.281 W/m^2 K. The results indicate that the PV-DSF has better performance than PV-IGU in reducing solar heat gains, while it has worse performance regarding thermal insulation. With a lower PV module temperature, the energy conversion efficiency of PV-DSF is 1.8% better than PV-IGU. Simulation models for the PV-DSF and the PV-IGU are developed and validated against experimental data. Using the validated models, the overall energy performances of PV-DSF and PV-IGU in five different climates of China are investigated. The results show that the average energy saving potential of the PV-DSF and the PV-IGU are 28.4% and 30%, respectively, compared to the commonly used insulating glass window in five different climates. On average, the performance of PV-IGU was 2% better performance than the ventilated PV-DSF in the five representative cities. However, if an appropriate ventilation control scheme was adopted, PV-DSF can have a much better performance than the PV-IGU. The models developed in this study can be used for selecting suitable PV windows in the design process, and the results achieved can be used as a guideline for utilizing PV windows in different climates.

Keywords: Building integrated photovoltaics, Semi-transparent photovoltaics, PV double skin façade, PV insulating glass unit, Building energy efficiency

© 2017. This manuscript version is made available under the CC-BY-NC-ND 4.0 license https://creativecommons.org/licenses/by-nc-nd/4.0/.

Nomenclature

G	heat flux rate (W/m^2)
m_i	measured data for the instance "i"
$\overline{m}$	average value of all measured data
N	number of data points
s_i	simulated data for the instance "i"
T	temperature (^{o}C)
U	heat transfer coefficient (W/m^2 K)

Abbreviation

a-Si	amorphous silicon
BIPV	building-integrated photovoltaics
COP	coefficient of performance
Cv(RMSE)	coefficient of root-mean-square error
DSF	double skin façade
HISG	heat insulation solar glass
IGU	insulating glass unit
MBE	mean bias error
MPP	maximum power point
PV-DSF	photovoltaic double skin façade
PV-IGU	photovoltaic insulating glass unit
SAPM	Sandia Array Performance Model
SHGC	solar heat gain coefficient
STPV	semi-transparent PV
WWR	window wall ratio

Subscripts

c	conductive
d	direct
i	indoor
o	outdoor
r	radiant
t	total

1. Introduction

With the development of industry and agriculture, the world has been consuming more and more energy. The extensive utilization of fossil fuels has resulted in a series of serious environment pollution problems [1-3]. To address these issues, renewable energies are competitively developed all over the world [4, 5]. As a representative, solar photovoltaic (PV) has been achieving a sharp growth during the last decades [6, 7]. Due to the limited space in urban areas, a good choice for PV technology application is to integrate PV technologies on buildings. This integration which is achieved by incorporating PV cells or modules with building envelope components such as roofing, siding, and glass is called building-integrated photovoltaic (BIPV) systems. Except for generating electricity in situ of buildings, BIPV systems also offer advantages in initial cost saving and aesthetic appearance because conventional construction materials are substituted by PV materials in new constructions [8].

In recent years, semi-transparent PV windows which can provide daylighting illuminance and generate electricity simultaneously have attracted the attention of many researchers. Fung et al. [9] developed a one-dimensional transient heat transfer model to evaluate the heat gain of semi-transparent photovoltaic modules for the building-integrated application. It was found that solar heat gain was the major component of the total heat gain. Lu and Law [10] investigated the overall energy performance of a single-pane semi-transparent PV window for office buildings in Hong Kong. The results showed that thermal performance was the primary consideration of energy saving in the entire system whereas electricity use of artificial lighting was the secondary one. The energy saving potential of semi-transparent PV windows was also reported by comparison with traditional glazings [11, 12]. However, as the high temperature of semi-transparent PV modules would lead to a thermal discomfort in the summer season, and the poor thermal insulation characteristic of single-pane PV windows would result in a severe heat loss in the winter season, it is a better choice to add an additional glass layer to form a multi-layer PV module, for example, PV insulating glass unit (PV-IGU) or PV double skin façade (PV-DSF). Fig. 1 shows the cross-section diagrams of the studied two PV windows. The additional glass layer and the air between the two layers can reduce heat transfer and decrease the cooling and heating loss through PV windows significantly.

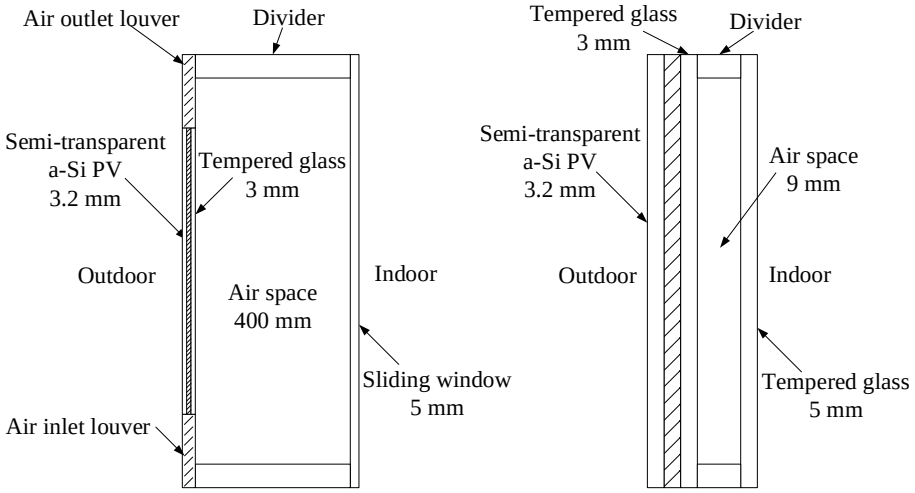

a) Structure of PV-DSF b) Structure of PV-IGU

Fig. 1. Cross-section diagrams of the PV-DSF and the PV-IGU.

PV-DSF consists of an outside layer of semi-transparent a-Si PV (a-Si STPV) panel, an inner layer of glass sheet as well as an intermediate air ventilation cavity. The air inlet and outlet louvers are installed below and above the PV modules, respectively. The cold air from the outside exchanges heat with the PV modules when going through the airflow duct and remove much waste heat from the cavity, which consequently reduces the operating temperature of solar cells. This ventilation effect not only reduces the building cooling load, but also improves the energy conversion efficiency of PV modules. A few studies on PV-DSFs were focused on the characteristics of ventilation in the cavity [13-15] and the impacts on energy performance [16-24]. Han et al. [7-9] investigated the heat transfer in the cavity of ventilated PV windows through numerical simulation. Various parameters affecting the local heat transfer coefficient of vertical glazing surfaces were evaluated. Chow et al. [16-18] compared the performances among a ventilated PV window, a single-pane PV window and an absorptive glazing window when installing on an office building in Hong Kong. It was found that the PV windows performed better on improving thermal comfort and reducing air conditioning demands, while their performance in lighting energy saving was worse. He et al. [19] compared the energy performance between a double-pane PV window and a single-pane PV window. The results revealed the superiority of the double-pane PV window to the single-pane PV window. Peng et al. [20, 21] developed a novel ventilated PV-DSF and evaluated its energy performance under different ventilation modes experimentally. A simulation model based on EnergyPlus was also developed to further evaluate the overall performance of the ventilated PV-DSF in different climates [22-24].

PV insulating glass unit (PV-IGU) consists of an outside layer of STPV panel, an air gap and an inner layer of a glass sheet. The air sealed in the air gap can increase the window's thermal insulation performance considerably. Compared to PV-DSFs, PV-IGUs possess the merits of simple installation and low cost, and hence are suitable for both new and retrofit buildings. The energy performance of PV-IGUs was also investigated by many scholars. Some studies focused on the influence factors of

energy performance. Miyazaki et al. [25] analyzed the effect of a PV-IGU on energy consumption of office buildings. The optimum solar cell transmittance and window to wall ratio (WWR) were obtained and the energy savings attributed to the PV-IGU was estimated. Wong et al. [26, 27] examined the power generation, thermal and visible light transmission performance of a poly-crystalline silicon PV-IGU experimentally and evaluated its overall energy performance via simulation. Song et al. [28] investigated the output power performance of a PV-IGU with considering the effects of both inclined slope and azimuth angle. Yoon et al. [29] studied the long-term temperature characteristics of a PV-IGU. Young et al. [30-33] proposed a heat insulation solar glass (HISG)-BIPV module and investigated its power generation, heat insulation, self-cleaning, wind pressure resistance and fire resistance performance separately. At last, there were also some researchers focused on the energy performance in different climates. Didone and Wagner [34] evaluated the energy saving potential of PV-IGUs on office buildings in Brazil. Ng et al. [35] analyzed the energy performance of PV-IGU in Singapore buildings. Chae et al. [36] evaluated the energy performance of PV-IGU in six different climates based on fabricated solar cell properties. Wang et al. [37] evaluated the energy performance of PV-IGU via numerical simulation and experimental tests in Hong Kong. Their results indicated that the energy performance of PV windows was determined by multiple parameters, such as thermal-optical characteristics of the window glazing system, building location, primary energy usage type, utility cost and the environmental impact factor of source energy type.

The above literature review showed that the energy performance of both PV-DSF and PV-IGU was investigated comprehensively, and their energy saving characteristics were verified by both experiments and simulation studies. However, the performance comparison between PV-DSF and PV-IGU was rarely reported. It is interesting to find out that in a certain climate which kind of PV windows would perform better and why that should happen. When comparing the two PV window technologies, PV-DSFs can usually reduce solar heat gain in the cooling season, while, PV-IGUs can reduce heat loss through windows in heating seasons by means of improving the thermal insulation performance. With different thermal characteristics, PV-DSFs and PV-IGUs have their own merits in different climate zones. Thus, the objective of this study is to compare the energy performance of PV-DSFs and PV-IGUs, and further investigate their applicability and energy saving potential in different climates of China. First, comparative tests have been carried out to compare the thermal, power and daylight performance of a PV-DSF and a PV-IGU in Hong Kong. Then, the simulation models were developed and validated against experimental data for the PV-DSF and the PV-IGU, respectively. Lastly, the validated simulation models were used to investigate the applicability and energy saving potential of PV-DSFs and PV-IGUs in different locations with different climatic conditions in China.

2. Experimental study

2.1 Test rig

To compare various performances of the PV-DSF and the PV-IGU, a BIPV test bed was built on a site office building in Hong Kong. Different performances, including thermal, power and daylight, were comparatively tested. As showed in Figure 2, the testbed was installed on the south-facing facade of the site office. The PV-DSF office has the same dimension as the PV-IGU office, which is 4 m (depth) × 2m (width) × 2.8 m (height). The whole PV array of the PV-DSF consisted of three semi-transparent a-Si PV modules; each module has a dimension of 1.25 m × 0.65 m. The PV-IGU only has one PV module and its dimension is 1.3 m × 1.1 m. The specifications of the two kinds of PV modules are showed in Table 1. These two kinds of PV modules had the same properties but different areas which resulted in the different voltages and maximum output power. The visual effects of both the PV-DSF and PV-IGU are illustrated in Figure 3. It is seen that both the PV-DSF and PV-IGU are see-through and people inside the room can see the outdoor scenery. Thus, both PV windows can provide well thermal performance, visual contact to the outdoor scenery and electricity generation simultaneously.

Fig. 2. PV-DSF and PV-IGU on the south-facing façade of the site office building.

Table 1 Specification of the PV modules.

Parameters	The PV module of PV-DSF	The PV module of PV-IGU
PV module area (m×m)	1.25 × 0.65	1.3 × 1.1
Short circuit current, I_{sc} (A)	1.24	1.23
Open circuit voltage, V_{oc} (V)	70	125
Current at maximum power point, I_{mp} (A)	0.95	0.96
Voltage at maximum power point, V_{mp} (V)	51.2	90.33
Maximum power under STC (Wp)	51	88
Efficiency, η (%)	6.3%	6.3%
Transmittance (%)	20%	20%

Fig. 3. The visual effect of PV-DSF (left) and PV-IGU (right) (from inside to outside).

Fig.4 showed the schematic diagram of the measurement setup. The instruments adopted in the testing campaign are showed in Fig.5, and their technical specifications are given in Table 2. A weather station was employed to record the weather data, including the ambient temperature and humidity, wind speed and direction, etc. Three pyranometers were used to measure the horizontal global and diffuse solar radiations and the south-facing incident solar radiation. A few temperature sensors and heat flux meters were used to measure the temperature and heat flux of the two PV windows for the purpose of evaluating their thermal performance. Two light meters were used to measure the daylight illuminance at the specific location (at the middle of the window in width, 2 m away from the windows, and 1 m in height) where represents the height of work surface in the two office rooms. The power generations of these two PV windows are recorded by two PV charging controllers, which can track the maximum power point (MPP) of PV windows and charge the battery system. The above data except for the output power data were collected by a data logger with a sampling interval of 1 min.

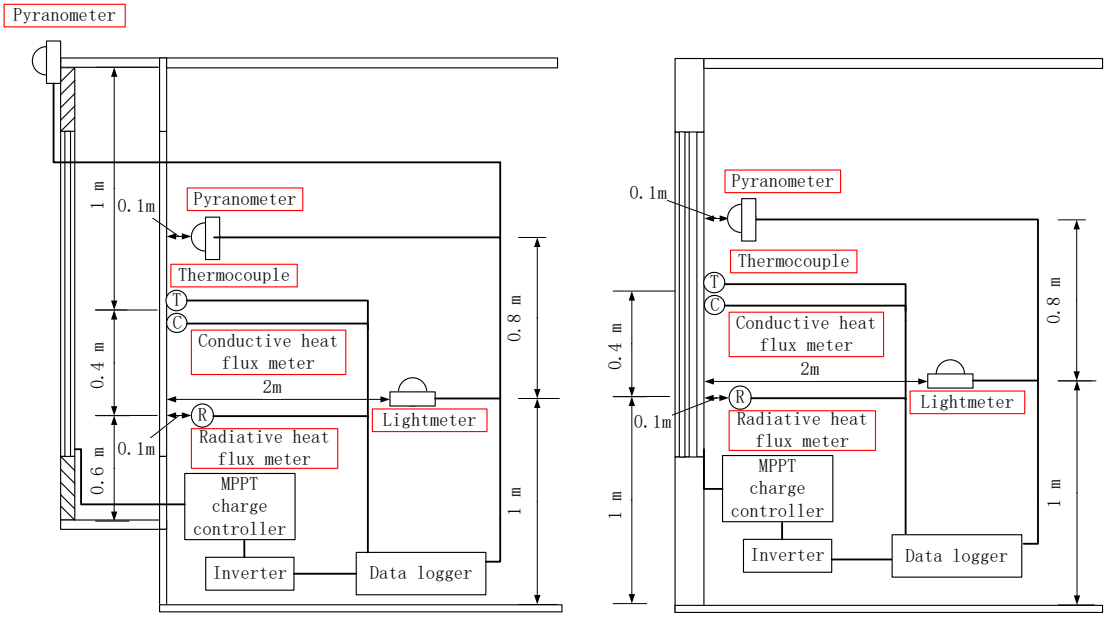

a) PV-DSF b) PV-IGU

Fig. 4. Schematic diagram of the measurement setup

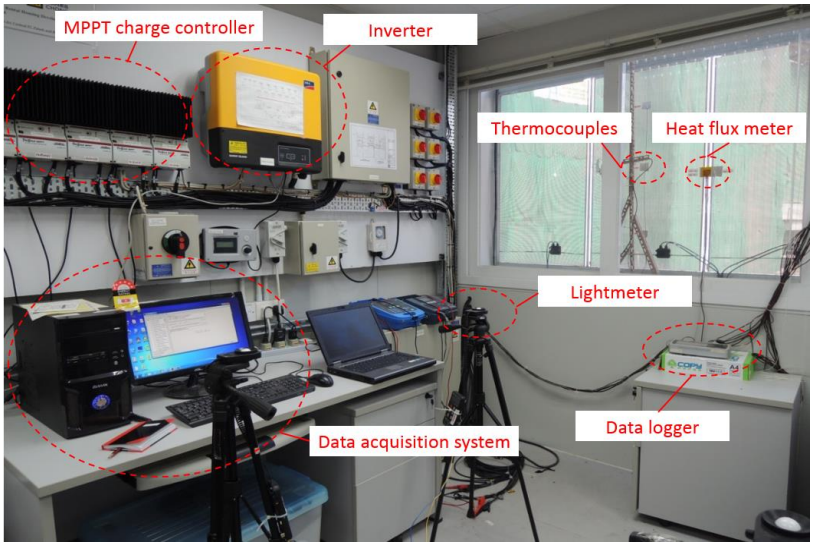

Fig. 5. Measurement instruments of the BIPV test bed.

Table 2 The key instruments and their specifications.

Equipment	Function	Manufacturer and model	Accuracy/sensitivity
Weather station	Weather condition recording	Thies Clima	Wind speed: 0.1m/s; Wind direction: 1°; Temperature: 0.1°C; Humidity: 0.1%;
Pyranometers	Solar irradiation measuring	EKO instruments (MS-802)	Sensitivity: about 7 μV/(W/m2); Non-linearity<0.2 % (at 1000W/m²);
Thermocouples	Temperature testing	RS Components (T type thermocouple)	Temperature range: -50 ~ 400°C; Accuracy: ±0.2°C;
Heat flux meter	Heat flux measuring	Captec Enterprise (RS-30)	Sensitivity: 2.0 μV/(W/m²); Response time: 0.3 seconds;
Lightmeter	Daylighting illuminance measuring	Casella	20 (M129005), 200, 2000, 20000, 200000 Lux
Inverter	Convert DC to AC power and record Power generation	SMA sunny island 2012	Max efficiency:93.6% Total output voltage harmonic distortion: 4%;
MPPT charge controller	Tracking Max power point	MORNINGSTAR TS-MPPT-30	Peak Efficiency 99%
Data logger	Data collection	Graphtec (GL820 Midi Data Logger)	The minimum resolutions are 1 μV and 0.1 °C;

The comparative tests were lasted for about 7 months from September 2014 to 30 April 2015. However, due to the failure of temporary power supply to the site office building, the experimental data in certain time periods was not collected or missed. Given the completeness and the good weather conditions, the experimental

data in January 2015 was chosen to compare the overall energy performance between the PV-DSF and the PV-IGU, as well as to validate the developed simulation models for each PV window. In Hong Kong, the weather of January is mostly sunny which is suitable for conducting performance comparison between PV windows.

2.2 Comparison of thermal performance

In this study, the two most popular indices for evaluating the thermal performance of building envelopes, i.e., solar heat gain coefficient (SHGC or g-value) and U-value, were used in comparison [38]. SHGC is the fraction of incident irradiance that enters through a window, which includes both the directly transmitted portion and the absorbed and re-emitted portion. [39]. U-value is the overall heat transfer coefficient from inside of a building to outside [40]. The difference is that SHGC shows how well the window prevents solar penetration, while U-value shows how well the window prevents heat loss. In this paper, experimental data was used to calculate the SHGCs and U-values of the PV-DSF and PV-IGU, respectively. Conductive heat flux meters and radiant heat flux meters were adopted to measure the conductive and radiant heat gains through the inside window, respectively. Also, three pyranometers were vertically installed outside and inside the rooms to measure the south-facing incident solar radiation and the direct solar radiations shining in the two indoor rooms, respectively. With the above data, the SHGC of the PV-DSF and PV-IGU were approximately calculated by the following equation:

$$\mathrm{SHGC} \approx \frac{(G_d+G_r+G_c)}{G_t} \tag{1}$$

where G_d is the direct solar radiation penetrating the window and shining over the indoor room, (W/m^2); G_r is the radiant heat flux from the inside window, (W/m^2); G_c is the conductive heat flux transferring from the inside window to the indoor room, (W/m^2); and G_t is the total incident solar radiation on the south-facing facade, (W/m^2).

Similarly, the U-value of PV-DSF and PV-IGU can be calculated by the following equation:

$$\mathrm{U}_{value} \approx \frac{(G_r+G_c)}{T_i-T_o} \tag{2}$$

where G_r is the radiant heat loss from the inside window to the outside at nights, (W/m^2); G_c is the conductive heat loss through the window, (W/m^2); T_i is the indoor air temperature, (^{o}C); T_o is the outside ambient air temperature, (^{o}C).

In this study, the SHGC was calculated only when the solar irradiance was higher than 200 W/m^2 for a complete hour [41], and the U-value was calculated only when the inside and outside temperature difference was larger than 2^{o}C. It meant that some unstable data was removed to reduce the calculation error. Figures 6 and 7 show the SHGCs, the heat losses and the U-values of the PV windows, respectively. Specifically, the average solar heat gain coefficients (SHGCs) of the PV-DSF and the PV-IGU were 0.152 and 0.238, respectively. The average U-values of the PV-DSF and the PV-IGU were found to be 2.535 W/m^2 K and 2.281 W/m^2 K, respectively.

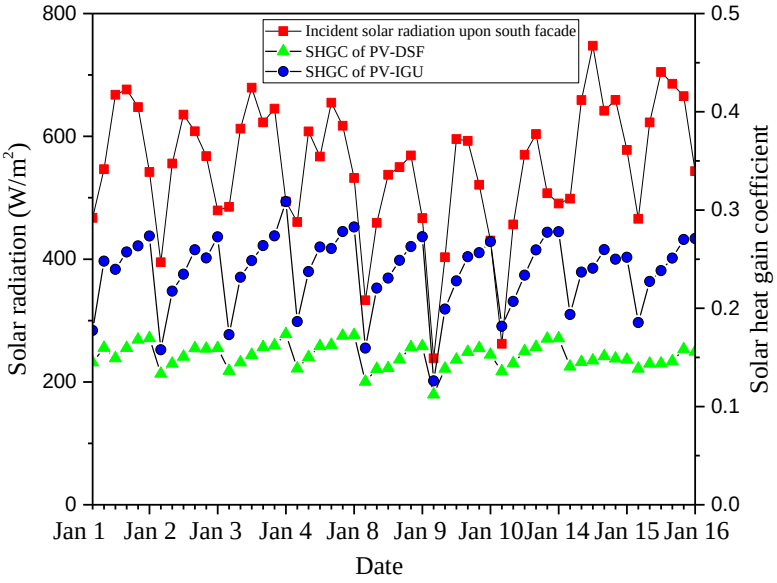

Fig. 6. Solar heat gain coefficients of the two kinds of PV windows.

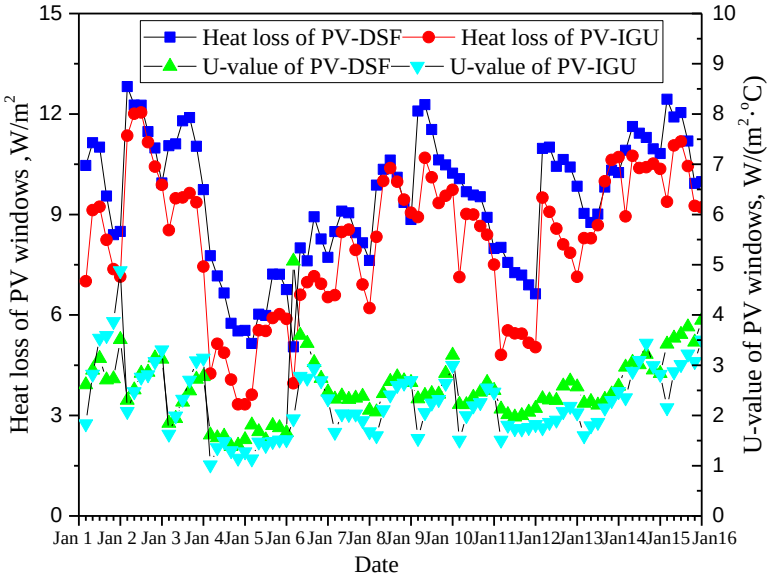

Fig. 7. Heat losses and U-value of the two kinds of PV windows.

2.3 Comparison of daylight performance

A comparison of daylight illuminance between the PV-IGU and the PV-DSF is showed in Fig. 8. As the office rooms were occupied on weekdays, the daylight comparative tests were carried out at weekends and holidays. It seems like that the daylight performance of the PV-DSF is better than the PV-IGU. However, given that the area of the PV-DSF is larger than the PV-IGU, the comparison results in Figure 8 might not be accurate. A comparison using the same dimension of PV windows should be conducted by simulation in the following section. On sunny days, the daylighting illuminance in the room mounted with PV-DSF reached 350 lux which can reduce a considerable amount of lighting energy use in combination with a dimmable lighting system. The daylighting illuminance in the room installed PV-IGU

reached 200 lux when the WWR is 26%. The window to wall ratio was defined as the ratio of the window area to the exterior wall area [42]. Usually, the larger the WWR is, the higher the daylight illuminance is. It can be expected that the daylight performance would be better when the WWR increases to 43% as the PV-DSF is.

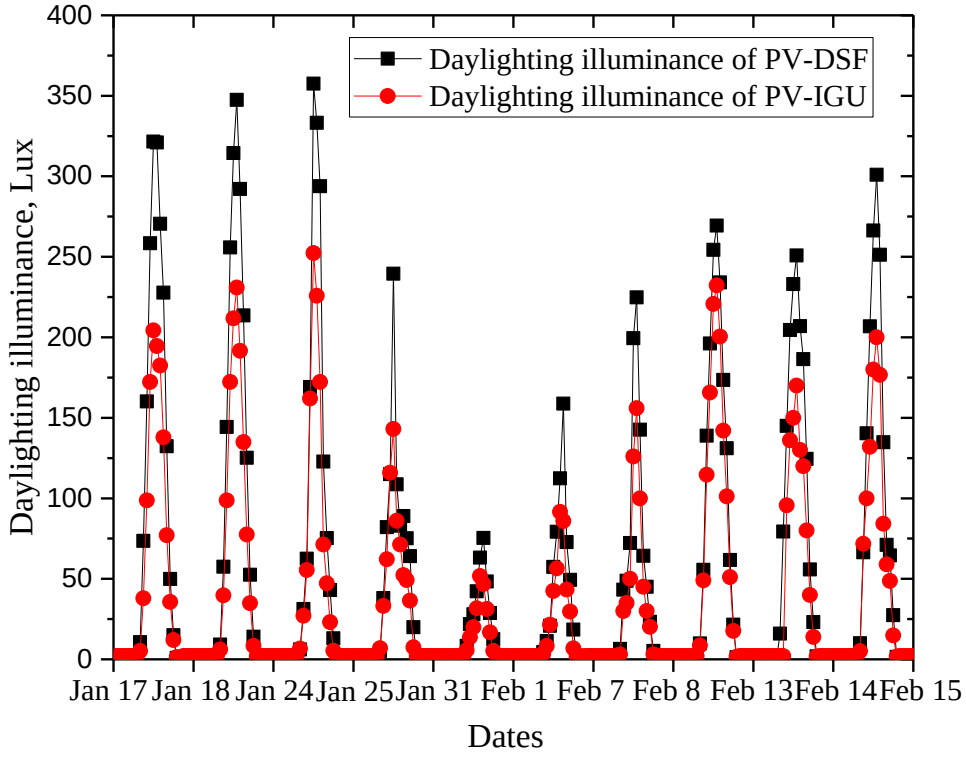

Fig. 8. Comparison of daylight illuminance.

2.4 Comparison of power generation performance

Fig. 9 presents the comparison of the daily power output of the two kinds of PV windows. It is seen that the maximum daily power outputs per unit area of the PV-DSF and the PV-IGU were 326.3 Wh and 320.6 Wh, respectively, occurred on 14 Jan. 2015. Considering the daily incident solar irradiance upon the south façade was 5771.7 Wh/m^2, the average energy conversion efficiency was 5.7% and 5.6%, respectively. These energy conversion efficiencies were lower than the efficiencies presented in Table 1 because the efficiencies in Table 1 were measured under the standard test conditions and the energy losses were not included. It is seen that the energy conversion efficiency of the PV-DSF was a little bit higher than the PV-IGU. The main reason was attributed to the lower temperature of PV modules for the ventilated PV-DSF, which consequently contributed a higher energy conversion efficiency. However, as the temperature difference was not too much, the difference in energy conversion efficiency was very little.

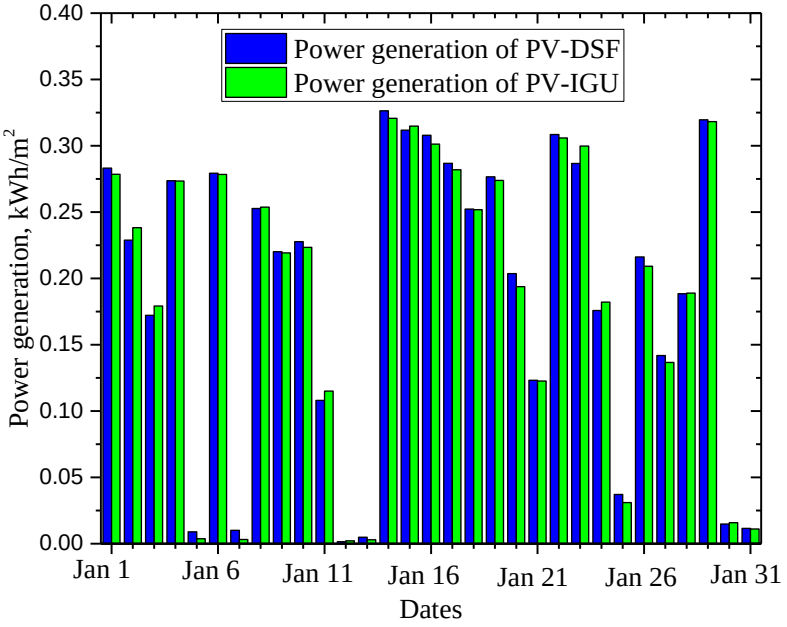

Fig. 9. Power output comparison of PV-DSF and PV-IGU.

3. Simulation models of PV-DSF and PV-IGU

3.1 Model development

To investigate the applicability and energy saving potential of PV-DSFs and PV-IGUs and in different climates, numerical simulation models based on EnergyPlus were developed to comprehensively investigate the overall energy performance of these two kinds of PV windows. The heat transfer model, daylighting model and PV power generation model in EnergyPlus were adopted to investigate the corresponding performance simultaneously. More detail of the simulation model could be found in the authors' previous research [37]. With the development of a-Si PV technology, the PV module used in this research could reach similar energy conversion efficiency with a higher transmittance compared to the former research. To accurately simulate the energy performance of STPV windows, the Sandia Array Performance Model (SAPM) was used. Previous studies have proved that the SAPM can model the energy performance of a-Si PV module with an acceptable accuracy [22]. The model development began with the test of the thermal, optical, and electrical characteristics of the PV module samples. The electrical characteristics under the standard testing conditions and the temperature coefficients were measured in the laboratory using a solar simulator. The other parameters, such as I-V curve and some key electrical characteristics (I_{sc}, V_{oc}, I_{mp}, V_{mp}, P_{max}), were measured in an outdoor testbed as shown in Figure 10. The testing data obtained from the indoor and outdoor measurements were used to determine the parameters which were imported into the SAPM model for power generation simulation. For validation, the weather data collected by the weather station was used. The developed simulation models in EnergyPlus are showed in Fig. 11.

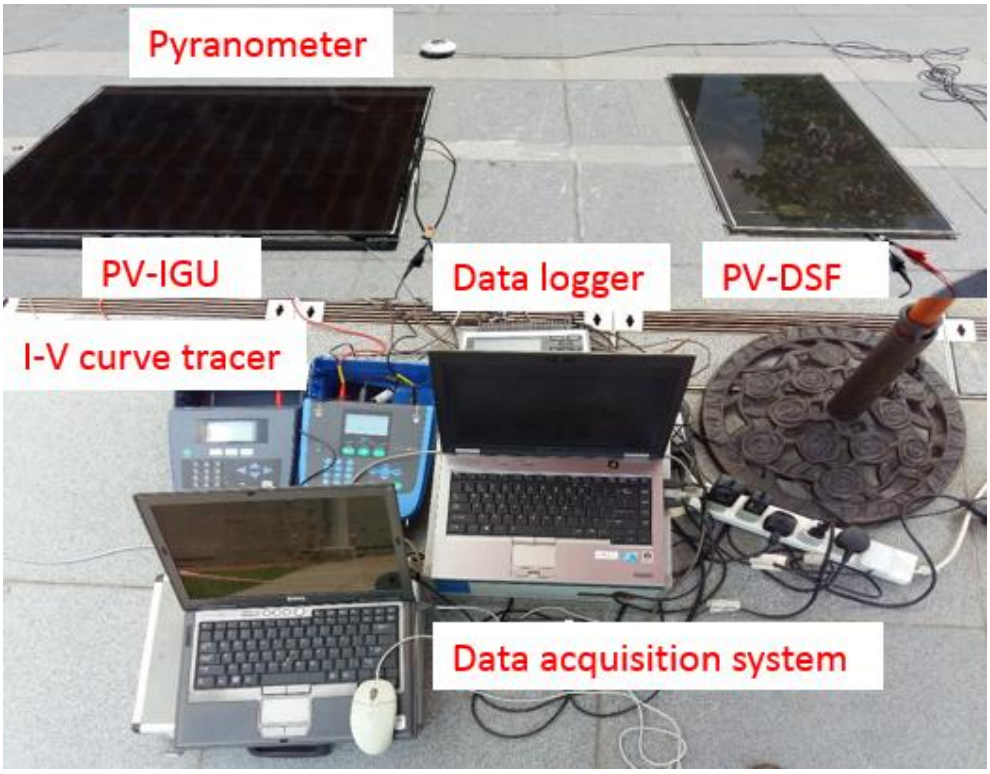

Fig. 10. Outdoor testing rig for determining SAPM parameters.

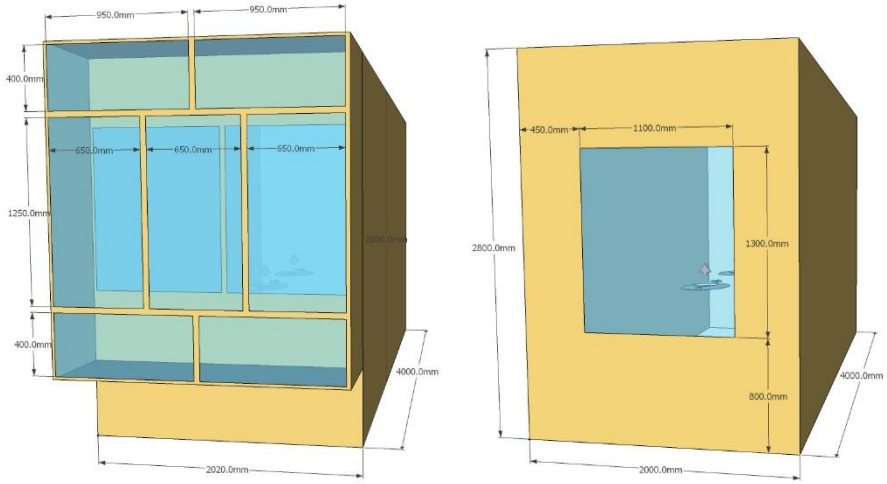

a) PV-DSF model b) PV-IGU model

Fig. 11. PV-DSF and PV-IGU models in EnergyPlus.

Two indices which have wide application in model validation were introduced to evaluate the models' accuracy. They are the mean bias error (MBE) and the coefficient of root-mean-square error (Cv(RMSE)). MBE and Cv(RMSE) can be calculated by Equation (3) and (4) as follows:

$$\mathrm{MBE}(\%) = \frac{\sum_{i=1}^{N}(m_i - s_i)}{\sum_{i=1}^{N}(m_i)} \tag{3}$$

$$\mathrm{Cv(RMSE)}(\%) = \frac{\sqrt{\left(\sum_{i=1}^{N}(m_i - s_i)^2/N\right)}}{\bar{m}} \tag{4}$$

where, m_i and s_i are the measured and simulated data for the instance "i",

respectively; N is the number of data points; $\overline{m}$ is the average value of all measured data.

A positive value of MBE indicates that the simulation result is higher than the experimental data and vice versa, while the Cv(RMSE) is a measurement of how close the simulated value is to the experimental output. As indicated in ASHRAE Guideline 14, if the MEB and Cv(RMSE) of a simulation model are lower than 10% and 30%, respectively, it is deemed to be acceptable in accuracy [43]. The data chosen to validate the simulation model started from Jan 16 to Jan 23, 2015. The global and diffuse solar irradiances on the horizontal surface are shown in Figure 12. It is seen that the first four days were sunny days, the following two days were cloudy, and the last day was a sunny day.

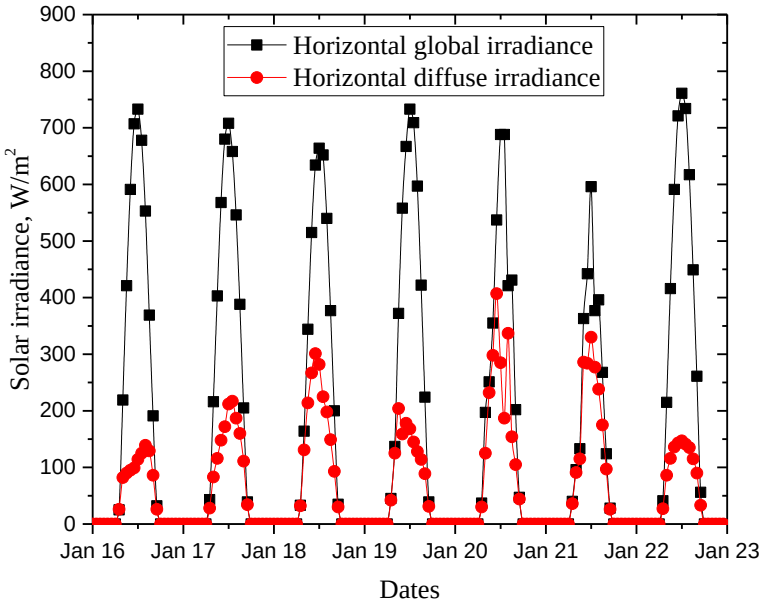

Fig. 12. Global and diffuse solar irradiances on the horizontal surface.

3.2 PV-DSF model validation

Comparison of the inner glass temperature, heat gains, daylighting illuminance, power generation of the simulated and measured values of the PV-DSF are illustrated in Figure 13. The MBE and Cv(RSME) of the inner glass temperature are -2.79% and 5.2%, respectively. This temperature is related to the heat gains coming through the PV windows to the indoor room. The accurate temperature prediction contributes an accurate prediction of heat gain of which the MBE and Cv(RSME) are -1.51% and 17.63%, respectively. As the lights were turned on to meet the lighting requirement for work on weekdays, the daylighting illuminance validations were only carried on weekends and holidays. The MBE and Cv(RSME) of daylighting illuminance are -1.53% and 28.38%, respectively. The daylighting illuminance on sunny days can reach up to about 300~400 lux, which gets close to the office illuminance requirement of 500lux [44]. The MBE and Cv(RSME) of power generation are -2.14% and 25.72%, respectively. The maximum power output per unit area was about 48 W/m^2 on sunny days. The average energy conversion efficiency was 5.6% for the studied PV-DSF. Since the MBE and Cv(RSME) of all above parameters are within the

regulated values of ASHRAE standard, the PV-DSF simulation model is considered to be acceptable in accuracy.

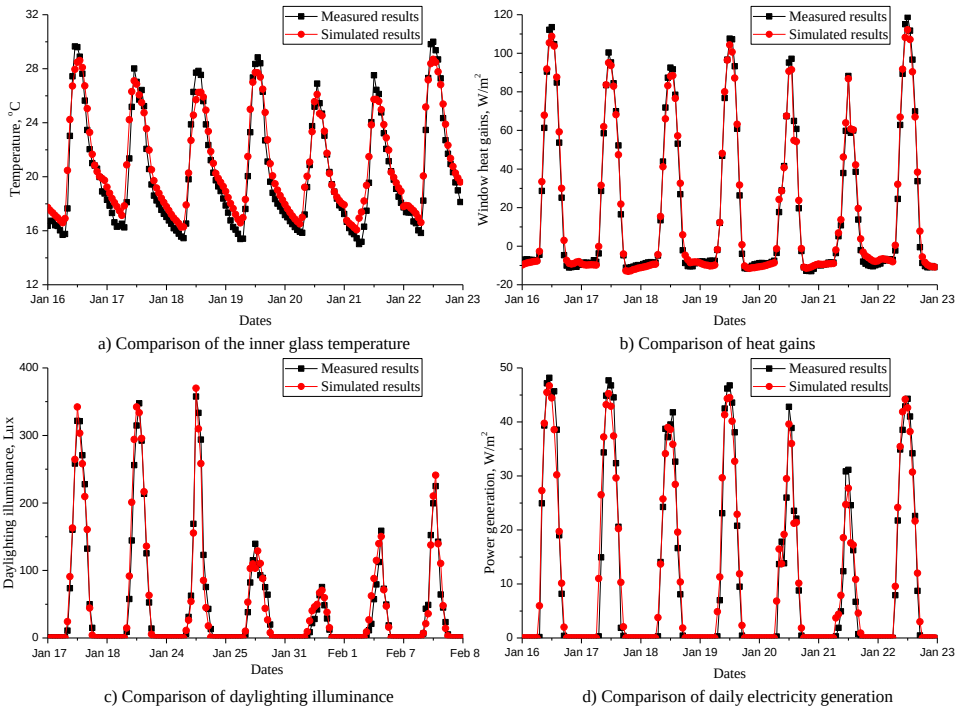

a) Comparison of the inner glass temperature

b) Comparison of heat gains

c) Comparison of daylighting illuminance

d) Comparison of daily electricity generation

Fig. 13. Comparison of measured data and simulated results of PV-DSF.

3.3 Model validation of PV-IGU

Figure 14 shows the validation results of the PV-IGU. The MBE and Cv(RSME) of PV temperature are -2.38% and 6.83%, respectively. The inner glass temperature of the PV-IGU was higher than that of the PV-DSF, the average temperature difference is 7.7°C. The higher inner glass temperature results in a larger heat flux, as a result, the average heat gain of the PV-IGU was higher than that of the PV-DSF by 37 W/m^2. The MBE and Cv(RSME) of heat gains of the PV-IGU are -4.43% and 19.17%, respectively. The MBE and Cv(RSME) of daylighting illuminance are -5.66% and 28.30%, respectively. The daylighting illuminance on sunny days can reach up to 300 lux. The illuminance values of the PV-IGU are lower than those of the PV-DSF, which was mainly due to the smaller size of the PV-IGU. The maximum power output per unit area of the PV-IGU is about 47 W/m^2. The MBE and Cv(RSME) of the power generation are -8.21% and 24.31%, respectively for the PV-IGU. The energy conversion efficiency is about 5.5% for this studied PV-IGU. Since the MBE and Cv(RSME) of all above parameters are within the regulated values of ASHRAE standard, it can be concluded that the developed simulation model are capable of simulating the energy performance of the PV-IGU.

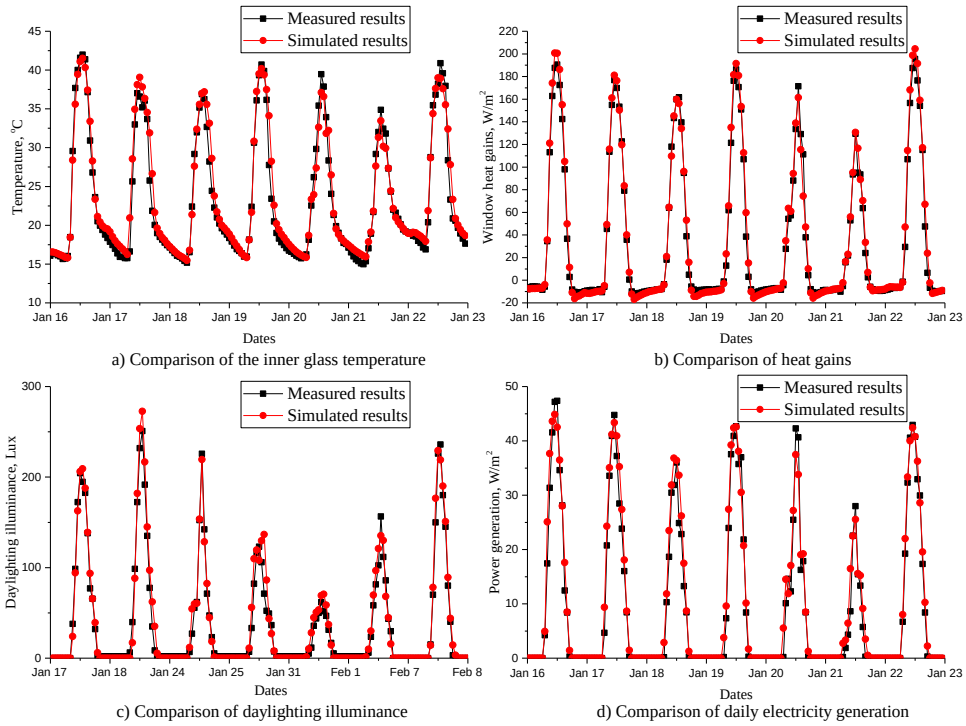

Fig. 14. Comparison of measured data and simulated results of PV-IGU.

4. Energy saving potential in different climates

From the above validation work, it is found that the developed simulation models are reliable for predicting the overall performance of the PV-DSF and the PV-IGU. Thus, the simulation models were adopted to further investigate the applicability and energy saving potential of the two PV windows in different climates of China. A typical office room, as shown in Figure 15, was chosen for the feasibility study of PV-DSF and PV-IGU in different cities. The area of the room is 18m^2, and the window to wall ratio (WWR) is 40%. All surfaces of the room are set to be interior wall except for the south surface, which was an external wall. On the south-facing external wall, 4 pieces of 1.3 m × 1.1 m PV windows were installed. The heating and cooling thermostat set points were 18 and 26 °C, respectively. A direct expansion cooling coil system (COP=2.78) was used for cooling and a gas boiler (heating efficiency is 0.8) was used for heating. A lighting load density of 9 W/m^2 was assumed, and a continuous lighting control model was used to regulate the artificial lighting output according to the variation of daylight illuminance. The air-conditioning system and lighting system were only operated during working time (from 8:00 AM to 5:00 PM). In order to accurately compare the annual energy consumption, the electricity energy use and gas energy use were converted into source energy use with the conversion coefficients of 3.167 and 1.084, respectively [45]. The source energy consumption takes all the transmission, delivery, and production losses of energy into account and represents the total amount of raw fuel consumption.

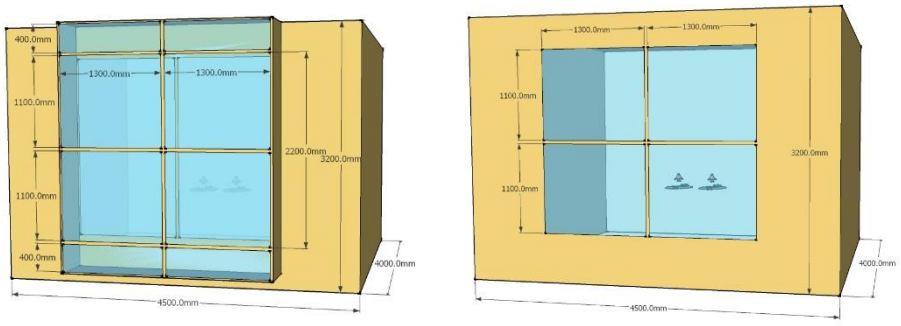

a) Office room model mount PV-DSF b) Office room model mount PV-IGU

Fig. 15. The developed office models with different PV windows.

According to the Chinese standard "Design standard for energy efficiency of public buildings" (GB 50189-2015) [46], China is divided into five climatic regions as follows, severe cold, cold, hot summer and cold winter, moderate, and hot summer and mild winter. Five cities, viz. Harbin, Beijing, Changsha, Kunming and Hong Kong, were selected to represent the five corresponding climatic zones. The U-value of the external wall was set according to the limit values of the energy-saving standard, which are showed in Table 3. To evaluate the energy efficiency of the studied PV windows, a conventional insulated glass window was used for baseline and comparison purpose. The U-value and SHGC of the conventional window were also determined according to the Chinese energy-saving standard.

Table 3 Summary of the adopted building envelope parameters.

Region	Representative	U-value of wall (W/m^2K)	Conventional insulated glass window	U-value of the conventional window (W/m^2K)	SHGC of the conventional window
Severe cold	Harbin	0.38	6 mm Clear+12 mm air+6mm Low-e	2.0	0.63
Cold	Beijing	0.50	6 mm Clear+6 mm air+6mm Low-e	2.2	0.62
Hot summer and cold winter	Changsha	0.60	6 mm Clear+3 mm air+6mm Low-e	2.6	0.62
Moderate	Kunming	0.80	6 mm Clear+1.5 mm air+6mm Low-e	3.0	0.61
Hot summer and mild winter	Hong Kong	0.80	6 mm Clear+1.5 mm air+6mm Low-e	3.0	0.61

The simulation results are showed in Figure 16. It was found that the PV windows have better performance than the conventional insulating glass window. This is because the SHGCs of the PV windows are much lower than the contrastive window. As a result, the cooling load was reduced significantly for the PV windows.

Averagely, the PV-DSF and the PV-IGU can save 28.4% and 30% energy, respectively, in the five different climate zones comparing to the contrastive conventional window. Among the five cities, both the PV-DSF and the PV-IGU achieved the maximum energy saving potentials in Kunming, with the energy use reductions of 46.9% and 44.8%, respectively. The energy saving performance of PV-DSF and PV-IGU were also remarkable in other climates with the minimum energy saving potential of 10.4% and 13.7% in Changsha. In general, the PV-DSF has better performance in reducing cooling energy consumption and increasing power generation than the PV-IGU, while the PV-IGU outperforms the PV-DSF in reducing heating and artificial lighting energy uses. Considering the overall energy performance, the PV-IGU and the PV-DSF have similar performance. The benefit of PV-DSF in cooling energy saving is offset by the higher heating energy consumption, and the daylighting performance of the PV-IGU is slightly better than the PV-DSF. Averagely, the overall energy performance of the PV-IGU is 2% better than the PV-DSF in the five cities.

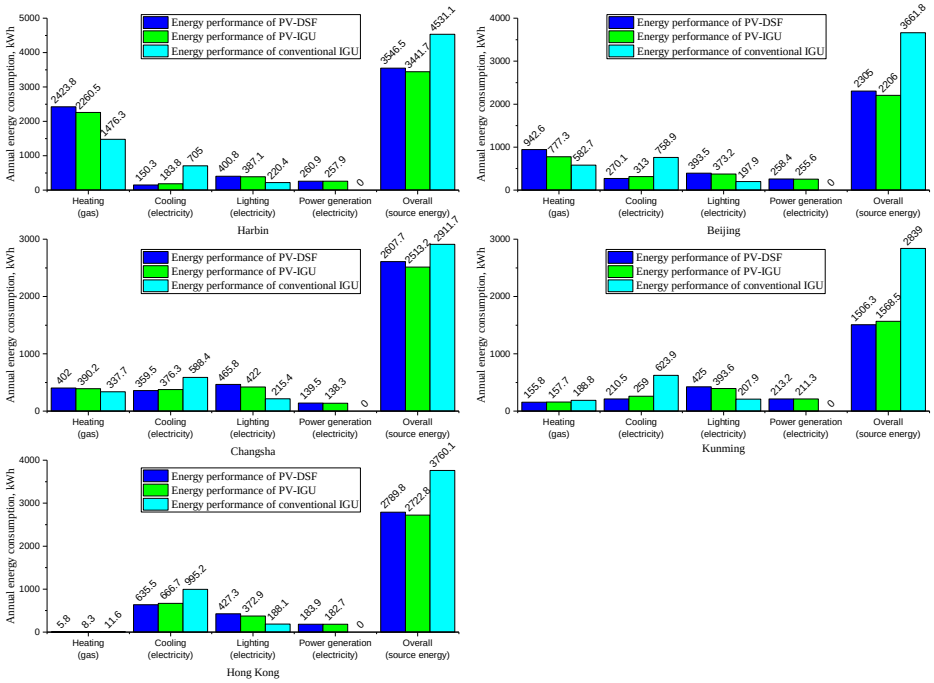

Fig. 16. Annual energy performance of the PV windows in different climates.

The inlet and outlet louvers of the PV-DSF were able to close to reduce heat loss through indoor rooms in the heating season. In this study, three different ventilation schemes were considered for the PV-DSF. The first scheme kept the louvers open all the year as discussed before, the second one was close the louvers all the year, and the last one was close the louvers in heating season only. As the heating energy consumption is dominant only in the severe cold climate and the cold climate. Thus, the different ventilation control schemes were only studied in these two climate zones. The urban centralized heating service was usually provided from Nov. 15 to Mar. 15 of the next year in Beijing. As Harbin has a colder climate than Beijing, the centralized heating service period is also longer, from Oct. 20 to Apr. 20 of the next year. The simulation results with different ventilation schemes are compared in Figure

17. It is seen that the energy performance of the PV-DSF varies with different control schemes. The difference of energy performance caused by different ventilation scenarios reached up to 8.7% and 10.5% in Beijing and Harbin, respectively. The energy performance of the PV-DSF with louvers open is worse than that of the PV-IGU in Beijing and Harbin. However, if close the louvers in the heating season only, the PV-DSF would outperform than the PV-IGU. The overall energy performance of the PV-DSF with an appropriate ventilation control is better than the PV-IGU by 4.5% and 7.7% in Beijing and Harbin, respectively. The results indicate that an appropriate ventilation and operation strategy is very important for the PV-DSF when it is applied in cold and severe cold climates. With an optimized operation scheme, the merits of the PV-DSF in reducing cooling load in summer and increasing the passive heating effect in winter can be maximized.

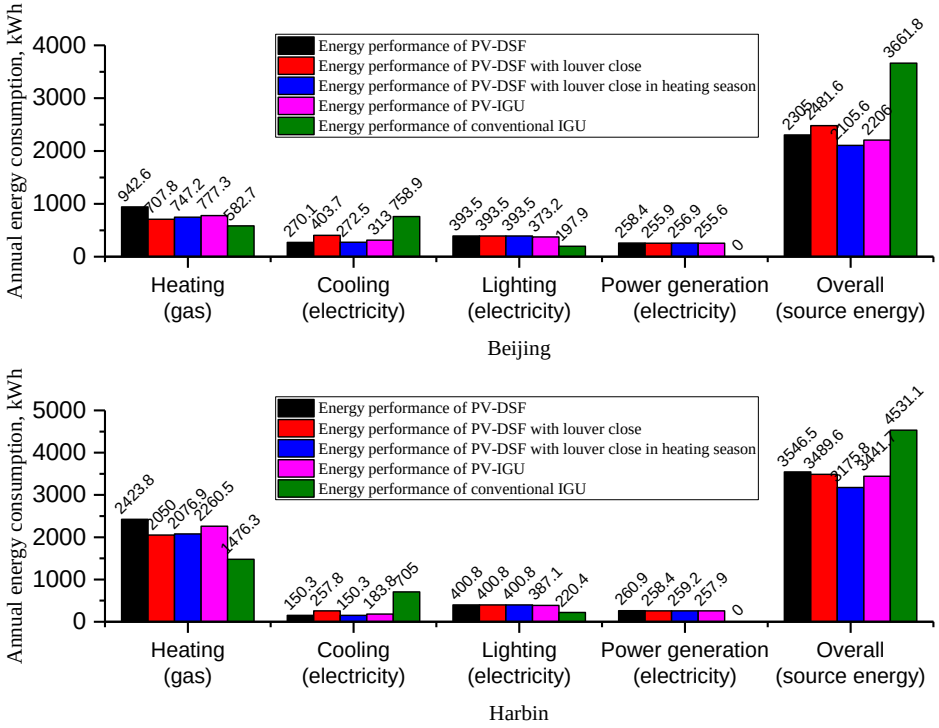

Fig. 17. Annual energy performance of PV-DSF with different control schemes.

The initial costs of the PV-DSF and PV-IGU were estimated to be HK$ 60/W and HK$ 50/W, respectively. Meanwhile, the rating power capacity of the PV windows adopted in this study is 62 W/m^2. The initial cost of the conventional insulating glass window is assumed to be HK$ 1500/m^2, so the incremental cost of PV-DSF and PV-IGU are HK$ 2220/m^2 and HK$ 1600/m^2, respectively. Taking the energy savings on the air conditioning and power generation into account, the annual electricity savings of PV-DSF and PV-IGU are 95 kWh/m^2 and 89.4 kWh/m^2, respectively. Assuming the residential tariff is HK$ 1.5 per kWh, the annual benefits of PV-DSF and PV-IGU are HK$ 143/m^2 and HK$ 134/m^2. As a result, the payback times would be 15.5 years and 12 years, respectively. The long payback time mainly be caused by the high initial cost of PV windows, but it is highly expected to be shortened with the PV cost reduction and efficiency improvement.

However, previous simulation results [36] also showed that the energy

performance of PV windows is affected by lots of variables, such as the weather condition, the building attribution, the window orientation, the service condition, the air conditioning system, etc. Thus, in practice, engineers should simulate the overall performance before making the decision to choose the PV window type. Although the simulation study was conducted in the five climate area in China, the simulation method could be used in other areas to investigate the performance of PV windows all over the world. On the whole, the simulation model developed in this study can be used for selecting suitable PV window technology, and the results obtained in this study could be a reference to a preliminary design scheme for PV windows.

5. Conclusions

In this paper, the energy performance of a PV-DSF and a PV-IGU were compared via experiment and simulation. Firstly, the experimental test was conducted to compare the thermal, daylight and power generation performance. It was calculated that the SHGC and U-value of the PV-DSF and PV-IGU in Hong Kong are 0.152 and 0.238, 2.535 W/m^2 K and 2.281 W/m^2 K, respectively. The results demonstrated that the PV-DSF is better than the PV-IGU in reducing solar heat gain, while the PV-IGU was better than the PV-DSF in thermal insulation. Then the simulation models of PV-DSF and PV-IGU were developed and validated against the experimental data. The simulation models were proven to have acceptable accuracy in predicting the energy performance of PV-DSF and PV-IGU. Lastly, the simulation models are used to further compare the performance of PV windows in different climate areas. Generally speaking, the PV windows performed better than the conventional insulating glass window in energy saving. The average energy saving potential of the PV-DSF and the PV-IGU were 28.4% and 30%, respectively. The overall energy performance of the PV-IGU was 2% better than the ventilated PV-DSF in the five representative cities. However, with the louvers closing in the heating season, the PV-DSF performed better than the PV-IGU. Thus, an appropriate operation strategy which could reduce the cooling load in summer and increase heat gain in winter is very important for PV-DSF especially in the cold and severe cold climate zones. However, since the energy performance of PV windows was related to lots of variables. It is recommended to simulate the overall performance of a real project before making a decision of choosing what kind of PV windows.

Acknowledgements

The authors appreciate the financial supports provided by the National Natural Science Foundation of China (Project No. 51608185), the Hong Kong Housing Authority Research Fund (Project No. K-ZJHE), the Fundamental Research Funds for the Central Universities (Hunan University, Project No. 531107040899), the China National Key R&D Program “Solutions to heating and cooling of buildings in the Yangtze river region” (Grant No. 2016YFC0700305) and Shenzhen Peacock Plan.

References

[1] IEA. World Energy Outlook Special Report 2016: Energy and Air Pollution. International Energy Agency (IEA). 2016.

[2] Nicoletti G, Arcuri N, Nicoletti G, Bruno R. A technical and environmental comparison between hydrogen and some fossil fuels. Energy Conversion and Management. 2015;89:205-13.

[3] Omer AM. Energy, environment and sustainable development. Renewable & Sustainable Energy Reviews. 2008;12:2265-300.

[4] Connolly D, Lund H, Mathiesen BV, Leahy M. A review of computer tools for analysing the integration of renewable energy into various energy systems. Applied Energy. 2010;87:1059-82.

[5] Li XW, Wen J, Malkawi A. An operation optimization and decision framework for a building cluster with distributed energy systems. Applied Energy. 2016;178:98-109.

[6] Tiwari GN, Mishra RK, Solanki SC. Photovoltaic modules and their applications: A review on thermal modelling. Applied Energy. 2011;88:2287-304.

[7] Sharma R, Tiwari GN. Technical performance evaluation of stand-alone photovoltaic array for outdoor field conditions of New Delhi. Applied Energy. 2012;92:644-52.

[8] Parida B, Iniyan S, Goic R. A review of solar photovoltaic technologies. Renewable & Sustainable Energy Reviews. 2011;15:1625-36.

[9] Fung TYY, Yang H. Study on thermal performance of semi-transparent building-integrated photovoltaic glazings. Energy and Buildings. 2008;40:341-50.

[10] Lu L, Law KM. Overall energy performance of semi-transparent single-glazed photovoltaic (PV) window for a typical office in Hong Kong. Renewable Energy. 2013;49:250-4.

[11] Li DHW, Lam TNT, Chan WWH, Mak AHL. Energy and cost analysis of semi-transparent photovoltaic in office buildings. Applied Energy. 2009;86:722-9.

[12] Liao W, Xu S. Energy performance comparison among see-through amorphous-silicon PV (photovoltaic) glazings and traditional glazings under different architectural conditions in China. Energy. 2015;83:267-75.

[13] Han J, Lu L, Yang HX. Thermal behavior of a novel type see-through glazing system with integrated PV cells. Building and Environment. 2009;44:2129-36.

[14] Han J, Lu L, Yang H. Numerical evaluation of the mixed convective heat transfer in a double-pane window integrated with see-through a-Si PV cells with low-e coatings. Applied Energy. 2010;87:3431-7.

[15] Han J, Lu L, Peng J, Yang H. Performance of ventilated double-sided PV facade compared with conventional clear glass facade. Energy and Buildings. 2013;56:204-9.

[16] Chow TT, Fong KF, He W, Lin Z, Chan ALS. Performance evaluation of a PV ventilated window applying to office building of Hong Kong. Energy and Buildings. 2007;39:643-50.

[17] Chow TT, Qiu ZZ, Li CY. Potential application of "see-through" solar cells in ventilated glazing in Hong Kong. Solar Energy Materials and Solar Cells. 2009;93:230-8.

[18] Chow TT, Pei G, Chan LS, Lin Z, Fong KF. A Comparative Study of PV Glazing Performance in Warm Climate. Indoor and Built Environment. 2009;18:32-40.

[19] He W, Zhang YX, Sun W, Hou JX, Jiang QY, Ji J. Experimental and numerical investigation on the performance of amorphous silicon photovoltaics window in East China. Building and Environment. 2011;46:363-9.

[20] Peng JQ, Lu L, Yang HX. An experimental study of the thermal performance of a novel photovoltaic double-skin facade in Hong Kong. Solar Energy. 2013;97:293-304.

[21] Peng JQ, Lu L, Yang HX, Ma T. Comparative study of the thermal and power performances of a semi-transparent photovoltaic facade under different ventilation modes. Applied Energy. 2015;138:572-83.
[22] Peng JQ, Lu L, Yang HX, Ma T. Validation of the Sandia model with indoor and outdoor measurements for semi-transparent amorphous silicon PV modules. Renewable Energy. 2015;80:316-23.
[23] Peng JQ, Curcija DC, Lu L, Selkowitz SE, Yang HX, Mitchell R. Developing a method and simulation model for evaluating the overall energy performance of a ventilated semi-transparent photovoltaic double-skin facade. Progress in Photovoltaics. 2016;24:781-99.
[24] Peng JQ, Curcija DC, Lu L, Selkowitz SE, Yang HX, Zhang WL. Numerical investigation of the energy saving potential of a semi-transparent photovoltaic double-skin facade in a cool-summer Mediterranean climate. Applied Energy. 2016;165:345-56.
[25] Miyazaki T, Akisawa A, Kashiwagi T. Energy savings of office buildings by the use of semi-transparent solar cells for windows. Renewable Energy. 2005;30:281-304.
[26] Wong PW, Shimoda Y, Nonaka M, Inoue M, Mizuno M. Field Study and Modeling of Semi-Transparent PV in Power, Thermal and Optical Aspects. Journal of Asian Architecture and Building Engineering. 2005;4:549-56.
[27] Wong PW, Shimoda Y, Nonaka M, Inoue M, Mizuno M. Semi-transparent PV: Thermal performance, power generation, daylight modelling and energy saving potential in a residential application. Renewable Energy. 2008;33:1024-36.
[28] Song J-H, An Y-S, Kim S-G, Lee S-J, Yoon J-H, Choung Y-K. Power output analysis of transparent thin-film module in building integrated photovoltaic system (BIPV). Energy and Buildings. 2008;40:2067-75.
[29] Yoon J-H, Shim S-R, An YS, Lee KH. An experimental study on the annual surface temperature characteristics of amorphous silicon BIPV window. Energy and Buildings. 2013;62:166-75.
[30] Young CH, Chen YL, Chen PC. Heat insulation solar glass and application on energy efficiency buildings. Energy and Buildings. 2014;78:66-78.
[31] Cuce E, Young CH, Riffat SB. Performance investigation of heat insulation solar glass for low-carbon buildings. Energy Conversion and Management. 2014;88:834-41.
[32] Cuce E, Young CH, Riffat SB. Thermal performance investigation of heat insulation solar glass: A comparative experimental study. Energy and Buildings. 2015;86:595-600.
[33] Cuce E, Riffat SB, Young CH. Thermal insulation, power generation, lighting and energy saving performance of heat insulation solar glass as a curtain wall application in Taiwan: A comparative experimental study. Energy Conversion and Management. 2015;96:31-8.
[34] Didone EL, Wagner A. Semi-transparent PV windows: A study for office buildings in Brazil. Energy and Buildings. 2013;67:136-42.
[35] Ng PK, Mithraratne N, Kua HW. Energy analysis of semi-transparent BIPV in Singapore buildings. Energy and Buildings. 2013;66:274-81.
[36] Chae YT, Kim J, Park H, Shin B. Building energy performance evaluation of building integrated photovoltaic (BIPV) window with semi-transparent solar cells. Applied Energy. 2014;129:217-27.
[37] Wang M, Peng J, Li N, Lu L, Ma T, Yang H. Assessment of energy performance of semi-transparent PV insulating glass units using a validated simulation model. Energy. 2016;112:538-48.
[38] Chow TT, Li C, Lin Z. Innovative solar windows for cooling-demand climate. Solar Energy Materials and Solar Cells. 2010;94:212-20.

[39] Marinoski DL, Güths S, Pereira FOR, Lamberts R. Improvement of a measurement system for solar heat gain through fenestrations. Energy and Buildings. 2007;39:478-87.
[40] Fokaides PA, Kalogirou SA. Application of infrared thermography for the determination of the overall heat transfer coefficient (U-Value) in building envelopes. Applied Energy. 2011;88:4358-65.
[41] Carlos JS, Corvacho H. Evaluation of the performance indices of a ventilated double window through experimental and analytical procedures: SHGC-values. Energy and Buildings. 2015;86:886-97.
[42] Goia F, Haase M, Perino M. Optimizing the configuration of a facade module for office buildings by means of integrated thermal and lighting simulations in a total energy perspective. Applied Energy. 2013;108:515-27.
[43] ASHRAE. ASHRAE Guideline 14-2014: Measurement of Energy Demand and Savings. Atlanta, GA, USA: American Society of Heating, Refrigerating and Air-Conditioning Engineers. 2014.
[44] CIBSE. Code for Lighting. Chartered Institution of Building Services Engineers, London. 2002.
[45] EnergyPlus. EnergyPlus 8.4. US Department of Energy: Washington DC, USA, 2014.
[46] National Standard of The People's Republic of China. Design standard for energy efficiency of public buildings, GB 50189-2015. Beijing (in Chinese)2015.